REPORT DOCUMENTATION PAGE

Form Approved
OMB NO. 0704-0188

1. AGENCY USE ONLY (Leave Blank)	2. REPORT DATE	3. REPORT TYPE AND DATES COVERED

4. TITLE AND SUBTITLE
Acoustic Absorption Measurements for Characterization of Gas Mixing

5. FUNDING NUMBERS
DAAD19-01-1-0571

6. AUTHOR(S) Aurelien Cottet, Graduate Research Assistant; Lei Wu, Post-Doctoral Fellow; Andrew Meyers, Research Engineer; David Scarborough, Research Engineer; Tim Lieuwen, Assistant Professor

7. PERFORMING ORGANIZATION NAME(S) AND ADDRESS(ES)
Georgia Institute of Technology
270 Ferst Drive
Atlanta, GA 30332

8. PERFORMING ORGANIZATION REPORT NUMBER

9. SPONSORING / MONITORING AGENCY NAME(S) AND ADDRESS(ES)
U. S. Army Research Office
P.O. Box 12211
Research Triangle Park, NC 27709-2211

10. SPONSORING / MONITORING AGENCY REPORT NUMBER
41297.1-EG

11. SUPPLEMENTARY NOTES
The views, opinions and/or findings contained in this report are those of the author(s) and should not be construed as an official Department of the Army position, policy or decision, unless so designated by other documentation.

12 a. DISTRIBUTION / AVAILABILITY STATEMENT
Approved for public release; distribution unlimited.

12 b. DISTRIBUTION CODE

13. ABSTRACT (Maximum 200 words)

This paper demonstrates the use of acoustic absorption measurements to characterize the level of molecular mixing between gaseous mixtures. This objective is motivated by the observation that many existing methods only quantify macro-scale entrainment. Over a large range of frequencies, acoustic damping is dominated by vibrational relaxation processes. Our approach takes advantage of the fact that the relaxation frequency for a particular gas is often a strong function of the other species it is in molecular contact with. Thus, the relaxation frequency of a dual component gas mixture varies with the level of molecular mixedness of the constituent species. We present the results of example calculations and experiments demonstrating the significant dependence of acoustic absorption levels upon mixing.

14. SUBJECT TERMS			15. NUMBER OF PAGES 8
			16. PRICE CODE
17. SECURITY CLASSIFICATION OR REPORT **UNCLASSIFIED**	18. SECURITY CLASSIFICATION ON THIS PAGE **UNCLASSIFIED**	19. SECURITY CLASSIFICATION OF ABSTRACT **UNCLASSIFIED**	20. LIMITATION OF ABSTRACT **UL**

AIAA-2003-3259

Acoustic Absorption Measurements for Characterization of Gas Mixing

Aurelien Cottet, Tim Lieuwen

Georgia Institute of Technology
Atlanta, GA

9th AIAA/CEAS Aeroacoustics Conference and Exhibit

12 - 14 May 2003

Hilton Head, SC

Acoustic Absorption Measurements for Characterization of Gas Mixing

Aurelien Cottet, Graduate Research Assistant
Lei Wu, Post-Doctoral Fellow
Andrew Meyers, Research Engineer
David Scarborough, Research Engineer
Tim Lieuwen, Assistant Professor

School of Aerospace Engineering
Georgia Institute of Technology
Atlanta, GA 30332-0150
Email: tim.lieuwen@aerospace.gatech.edu
PH: (404)894-3041
Fax: (404)894-2760

Abstract

This paper demonstrates the use of acoustic absorption measurements to characterize the level of molecular mixing between gaseous mixtures. This objective is motivated by the observation that many existing methods only quantify macro-scale entrainment. Over a large range of frequencies, acoustic damping is dominated by vibrational relaxation processes. Our approach takes advantage of the fact that the relaxation frequency for a particular gas is often a strong function of the other species it is in molecular contact with. Thus, the relaxation frequency of a dual component gas mixture varies with the level of molecular mixedness of the constituent species. We present the results of example calculations and experiments demonstrating the significant dependence of acoustic absorption levels upon mixing.

Introduction

This paper demonstrates the use of acoustic absorption measurements to characterize the level of molecular mixing between gaseous mixtures. This objective is motivated by the observation that many existing methods only quantify macro-scale entrainment. Capabilities for measuring molecular levels of mixedness are needed for various applications; e.g., in low emissions combustion systems where complete fuel-air mixing is needed to minimize NOx production. The particular approach we are pursuing uses measurements of acoustic absorption at a number of frequencies.

Acoustic waves propagating through a gaseous media are damped by absorption processes so that their amplitude continuously decreases. These absorption processes arise from viscosity, thermal conductivity and the relatively slow relaxation of the vibrational modes of gas molecules[1]. Vibrational relaxation processes damp acoustic waves through the following mechanism: the gas compression associated with the acoustic wave cause perturbations in the gas temperature and, thus, local translational energy. Through molecular collisions, the translational energy is redistributed to the rotational and vibrational degrees of freedom. During very low frequency acoustic perturbations, energy is fed from the translational to the vibrational energy modes of the gas during the compressive phase of the acoustic cycle. This energy is then returned from the vibrational to the translational energy modes during the rarefaction phase of the cycle. While gas translational and rotational modes equilibrate very quickly (generally within a few collisions), the vibrational mode requires extensively longer (several thousand collisions). Thus, even at relatively low frequencies the internal energy exchange processes cannot respond sufficiently quickly to acoustic fluctuations, with the affect that energy is not removed from or returned to the dilatational disturbance in phase with its oscillations. These nonequilibrium affects cause the acoustic wave to be damped. Maximum acoustic damping per wavelength of acoustic propagation distance occurs at the "relaxation frequency", f_v (the inverse of the characteristic vibrational relaxation time), whose exact value depends upon the molecular species. An additional, relatively minor, affect of these nonequilibrium phenomenon is that the speed of sound slightly increases with frequency. Following Pierce[2], Figure 1 plots the dependence of the acoustic absorption and sound speed upon normalized frequency, f/f_v.

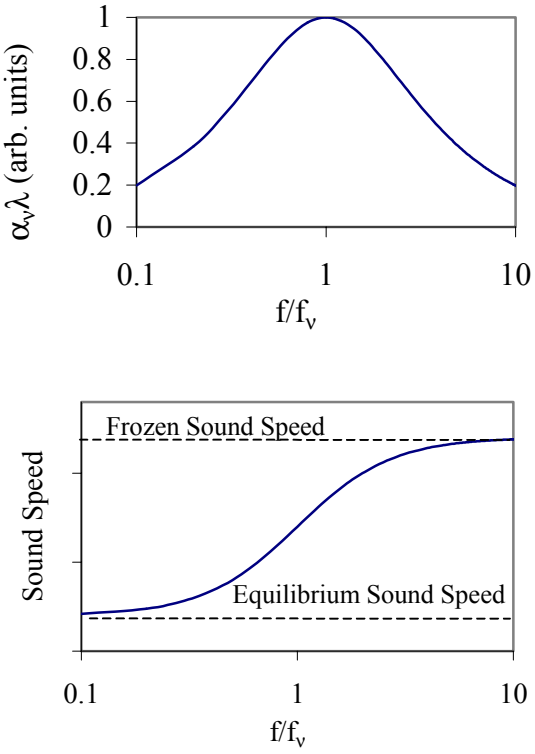

Figure 1. Dependence of the acoustic absorption and sound speed upon the normalized frequency.

In the figure, the quantity α_v refers to the acoustic damping coefficient due to vibrational relaxation; i.e., a wave propagating through a distance x is reduced in amplitude by the factor $\exp(-\alpha_v x)$. Figure 1 shows that acoustic wave damping due to vibrational relaxation is maximum at the relaxation frequency, f_v, and is reduced at higher and lower frequencies. The figure also shows that the speed of sound increases from its "equilibrium value" for $f << f_v$ to its "frozen value" when $f >> f_v$. In general this change in sound speed is quite small; i.e., a typical change is on the order of 0.1% of the nominal sound speed. The damping of acoustic waves by these vibrational relaxation processes is quite significant, however. *In fact, it is generally the dominant damping mechanism in gaseous media over a wide range of frequencies*. For example, Figure 2 plots the dependence of the acoustic damping factor, $\alpha\lambda$, upon frequency in air[2].

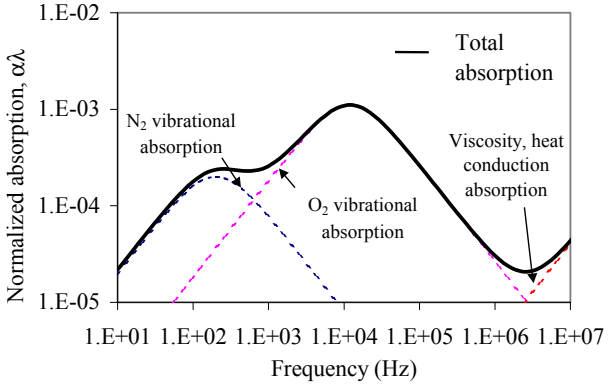

Figure 2. Dependence of acoustic absorption in air upon frequency. Calculation was performed assuming a room temperature, atmospheric pressure ambient environment, with a relative humidity of 20%.

Note that the plot decomposes the total damping into the relative contributions of N_2 vibrational relaxation, O_2 vibrational relaxation, and classical viscous and heat conduction processes. N_2 vibrational relaxation is the dominant damping source for frequencies up to a kilohertz, O_2 vibrational relaxation is dominant from one kilohertz up to about a megahertz, and viscosity and heat conduction are the most significant at higher frequencies.

The fundamental principle motivating this study is the fact that the *relaxation frequency of a particular gas is often a function of the other species with which it is in molecular contact*. Numerous studies have demonstrated this point in various gases, such as nitrogen[3,4], oxygen[5,6], carbon monoxide[7], and carbon dioxide[8]. As such, the relaxation frequency of a binary gas mixture varies with the level of molecular mixedness of the constituent species. In other words, if the two gases are completely unmixed, the vibrational relaxation rates of each species are simply equal to their value when alone. In contrast, if the gases are mixed, the relaxation frequency may have a different value that depends upon the relative constituent concentrations.

CO_2-H_2O Mixture Absorption Characteristics

Carbon dioxide-water vapor mixtures were chosen as the primary gases in this study. Carbon dioxide was chosen because of its relatively low vibrational temperature (~950 K), resulting in high levels of absorption at room temperatures. Many other candidate species with higher vibrational temperatures (e.g., N_2 or O_2) have low levels of vibrational mode excitation at room temperature, making the total amount of absorption relatively small over distances on the order

of our experiment size, ~0.18 m. Water was chosen as the second gas because of its strong impact on the vibrational relaxation rate of carbon dioxide. This is apparently due to the near coincidence of their first bending mode frequencies, resulting in very rapid V-V energy transfer rates. To illustrate, Figure 3 plots the dependence of the vibrational relaxation frequency, f_v, upon the amount of ambient water vapor and several other molecules. It shows that f_v in CO_2 with 0 and 0.1% H_2O increases from 20 to 150 kHz.

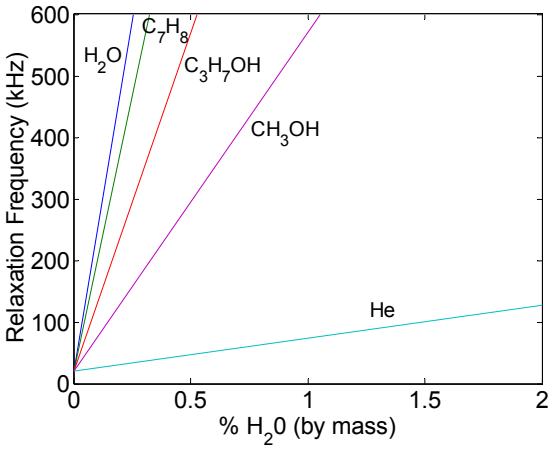

Figure 3. Dependence of f_v in carbon dioxide mixtures with the indicated species. Data obtained from Knudsen and Fricke[9].

Using the formula's presented by Pierce[2] for acoustic absorption as a function of temperature, Prandtl number, vibration temperature, and relaxation frequency, the total acoustic absorption (due to translational, rotational, and vibrational relaxation) were calculated. Plots of the dependence of the absorption coefficient upon frequency and water vapor concentration are shown below.

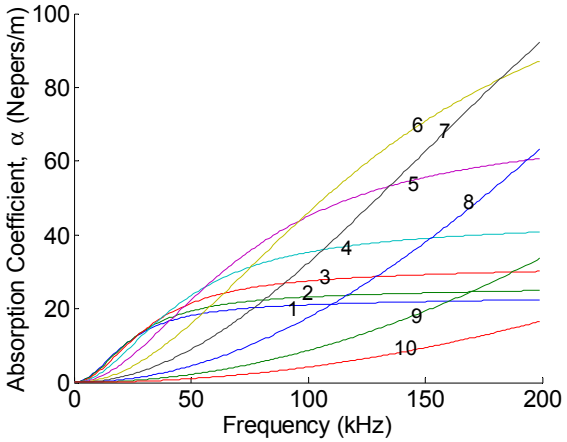

Figure 4. Dependence of total acoustic absorption coefficient upon frequency for several CO_2-H_2O mixtures; curves numbered to indicate H_2O levels of 0.001, 0.002, 0.005, 0.01, 0.02, 0.05, 0.1, 0.2, 0.5, and 1% by mass.

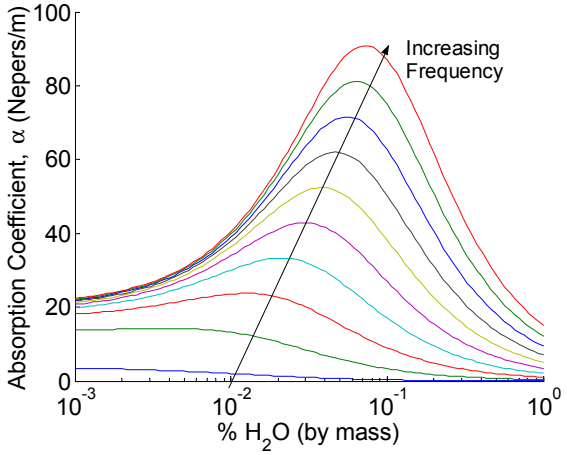

Figure 5. Dependence of total acoustic absorption coefficient upon H_2O concentration at frequencies of 10, 30, 50, 70, 90, 110, 130, 150, 170, and 190 kHz.

The figures show the monotonic increase in absorption coefficient magnitude with frequency, as well at its nonmonotonic and nonlinear dependence upon water vapor level.

Because of signal/noise considerations, the total amount of absorption must not be negligible nor too large; e.g., it is difficult to distinguish between a disturbance with a level 99.9% and 99% of its original value in the former and 0.001% and 0.0001% in the latter cases. As such, the optimal frequency range for absorption measurements depends upon the spatial distance between the source and receiver. The figures below plot the total absorption, $\exp(-\alpha x)$, across a distance x=0.18 m, corresponding to the size of the experiment described in the next section.

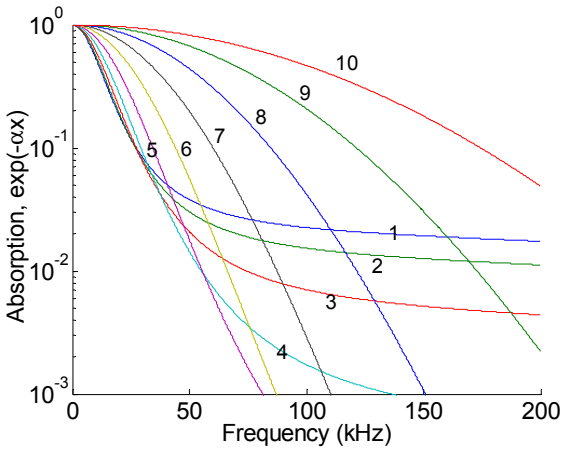

Figure 6. Dependence of total acoustic absorption, exp(-αx), across a distance x=0.18 m upon frequency for several CO_2-H_2O mixtures; curves numbering same as in Figure 4.

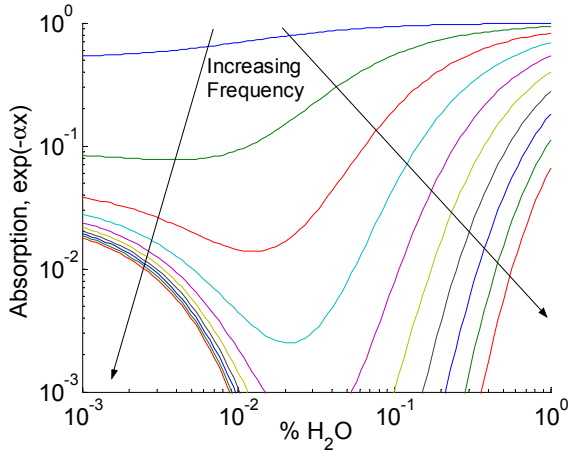

Figure 7. Dependence of total acoustic absorption, exp(-αx), across a distance x=0.18 m upon H_2O concentration at frequencies of 10, 30, 50, 70, 90, 110, 130, 150, 170, and 190 kHz.

The nonlinear dependence of absorption coefficient upon (in this case) water vapor content is key to the technique being pursued here. Because of this nonlinearity, the total absorption of a sound wave traversing the medium depends upon the local concentration values, and not just the integrated sum across the line of sight. If these relations were purely linear, the absorption coefficient would not change with mixedness levels. In addition, this nonlinearity allows for the approximate inversion of spatial mixedness profiles from measurements at multiple frequencies as we show below. To illustrate, consider a spatially inhomogeneous mixture of CO_2 and H_2O, where the spatial profile of the H_2O is plotted in Figure 8.

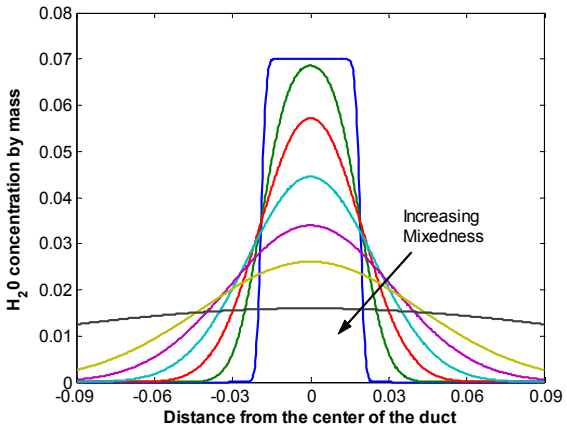

Figure 8. Assumed spatial dependence of H_2O mixedness level for model problem. Line points in the direction of increased mixedness.

Figure 9 plots the variation of absorption across a distance x=0.18 m with mixedness levels at several frequencies. The mixedness value indicated in the figure was computed by linearly scaling the ratio of the profile's standard deviation to its mean, σ/μ, between zero and unity.

At each frequency, the absorption level is normalized by its value in the perfectly mixed case. We use the integrated absorption $\exp(-\int \alpha dx)$ to determine the total absorption and assume negligible acoustic reflections. The figure shows that rather large differences exist (factors up to ~30) between the wave amplitude in the perfectly mixed and unmixed cases. These differences become quite small, however, at mixedness levels above about 75%.

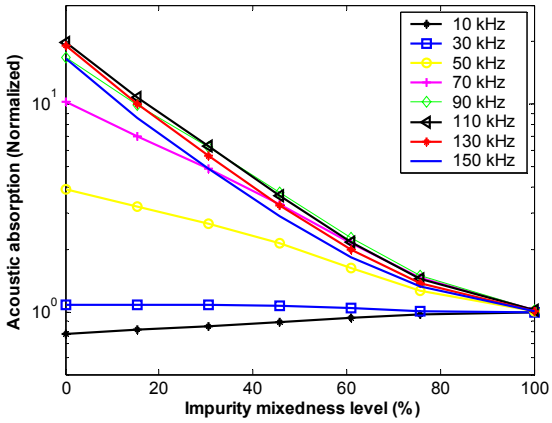

Figure 9. Dependence of acoustic absorption, $\exp(-\int \alpha dx)$, upon mixedness levels at frequencies of 10, 30, 50, 70, 90, 110, 130, and 150 kHz.

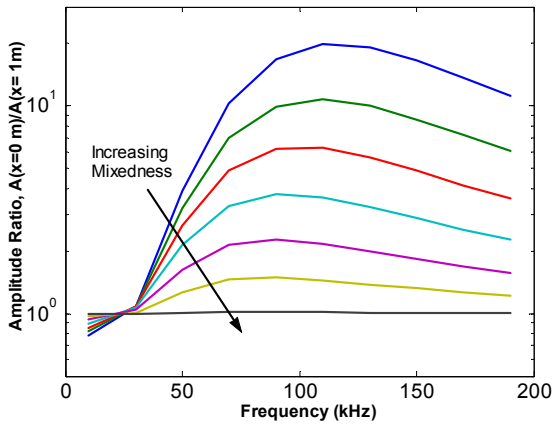

Figure 10 Dependence of acoustic absorption, $\exp(-\int \alpha dx)$, upon frequency at different mixedness levels; mixedness level same as in Figure 8.

The figures above clearly demonstrate that differences in acoustic absorption occur in the gas mixture with different mixedness levels. In order to assess the capability of absorption measurements to determine spatial mixedness profiles, we developed an inversion technique and applied it to this model problem. The profile used for the model problem is the same as in Figure 8 and was used because of its close relationship to that in our experimental facility. This gas mixture profile IP is a function of three parameters: low concentration percentage L_p, high concentration percentage H_p, and width, D.

$$IP = L_p + \frac{H_p - L_p}{2}\left[erf\left(\frac{W/2 - x}{D}\right) - erf\left(\frac{-W/2 - x}{D}\right)\right] \quad (1)$$

where W is the duct width, x is the distance from the center of the duct, and erf is the error function. Note that Eq. (1) is the solution of the 1-D diffusion equation with a finite line source.

The objective of the inversion approach is to determine the three parameter values: L_p, H_p, and D from absorption measured at three or more frequencies. As in our experiments, the acoustic amplitude $A(f)$ is normalized by its value in the perfectly mixed case, $A_{avg}(f)$, at each frequency to eliminate diffraction/reflection effects, then compared with the corresponding theoretical value. We determine the above three parameters by minimizing the following objective function:

$$\Delta(L_p, H_p, D) = \sum_f \left[\log\left(\frac{A(f)}{A_{avg}(f)}\bigg|_{\exp} \right) - \log\left(\frac{A(f, L_p, H_p, D)}{A_{avg}(f)}\bigg|_{th} \right) \right]^2 \quad (2)$$

The logarithm of the amplitude ratios is applied in this expression so that the normalized acoustic amplitude at each frequency is more equally weighted in the residue, Δ.

This inversion is complicated by the highly nonlinear character of the solution space which contains numerous local extrema. We used the downhill simplex method[10] to search for the values of the three parameters L_p, H_p, D that minimize the residues at all measured frequencies. It requires only function evaluations, not derivatives and is based on simple geometric operations. It is discussed in detail in Reference [11]. The inversion procedure is summarized in the flowchart in Figure 11.

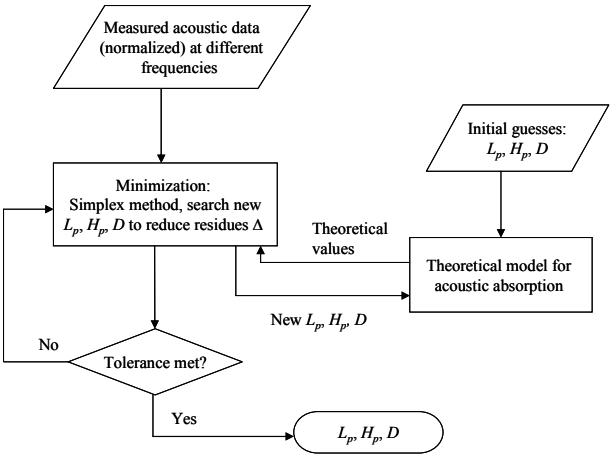

Figure 11. Flow chart for the inversion procedures.

In order to assess the sensitivity of this inversion procedure to uncertainty and noise, numerical simulations were performed. Theoretical "data" at 13 equally spaced different frequencies (30-150 kHz), such as are plotted in Figure 9, were calculated for given values of L_p, H_p, and D. Uniformly distributed, random noise of varying amplitude were added to these absorption data, which were then used as inputs for the inversion procedure to determine the values of the three parameters. For each percentage error, the inversion program was repeated fifty times with different random errors. The standard deviation of the estimate of the inverted parameter was then determined from these fifty ensembles. Figure 12 shows that the sensitivity of the inversion procedure is around unity; i.e., 10% errors in measurement translate into 5-10% errors in parameter estimates.

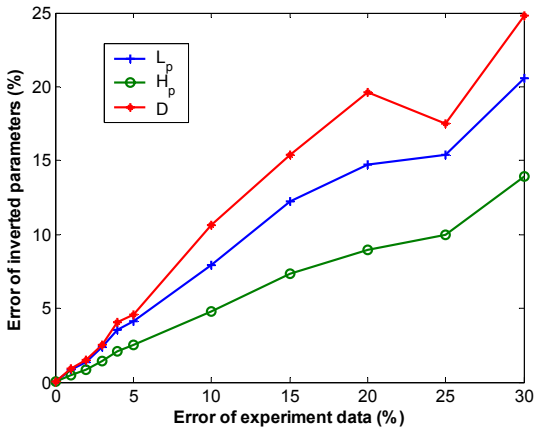

Figure 12. Sensitivity of inverted parameters to the noise in the experiment.

These results demonstrate the feasibility of the proposed technique. The following section describes an experimental facility and measurements that were performed to experimentally assess the technique.

Experimental Facility and Results

Having demonstrated the theoretical feasibility of gas mixedness characterization using acoustic absorption measurements, we have assembled a facility to experimentally demonstrate the technique. A photograph and drawing of the facility are shown in Figure 13. It consists of an 8-foot long, 8 x 11 inch section aluminum duct that is capped at one side and open at the other side. A box with one open end slides inside the duct. Two gases of arbitrary composition, denoted as Gas A and Gas B, flow through the main chamber and the translating box.

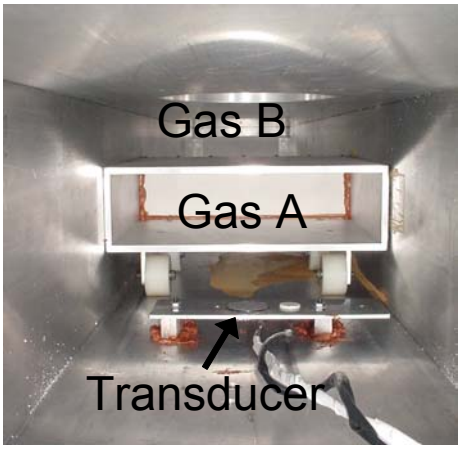

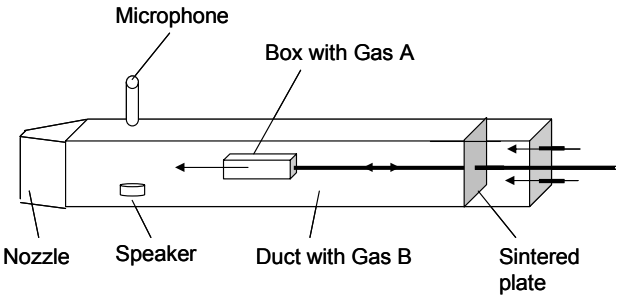

Figure 13. Photo (flow coming out of page) and drawing of facility developed for acoustic absorption measurements.

For this experiment, gases "A" and "B" simply consisted of two CO_2 sources with different levels of water vapor. Dry, industrial grade CO_2 (99.98% purity, < 10 ppm water vapor) flows through the main part of the box (Gas A). Gas B is humidified by passing the same grade CO_2 through a bubbler. The humidity of the gas is varied by mixing the relative concentrations of this stream with a second dry stream. Water/carbon dioxide mass ratios of 0-0.3% were achieved with this arrangement. The two gas flows are metered with velocities from 1cm/s to 5cm/s. These velocities and lengths were based on diffusive mixing calculations, with the requirement that the two gases could be completely mixed when the box is positioned the farthest distance from the transducer. As such, the degree of gas mixing can be varied via the box location and/or the gas velocity. The water vapor concentration was measured with a Tri-Sense relative humidity sensor, model EW-37000-00.

25 kHz to 65kHz acoustic signals are generated with a 38mm diameter, type 616341 electrostatic polaroid transducer Acoustic measurements are obtained with a 1/8" type 4191 Bruel and Kjaer microphone. The speaker and microphone are situated near the nozzle end of the duct.

In the experiment, two initially unmixed gas streams enter the duct from upstream. As these gases convect down the duct and mix, the acoustic absorption at different axial locations are measured. At each frequency the acoustic amplitude, $A(f)$, is measured as a function of the box position. The gas is acoustically interrogated by bursts of 10-50 acoustic cycles at the desired frequency, followed by a pause in order to allow the reverberant field to damp out, see Figure 14.

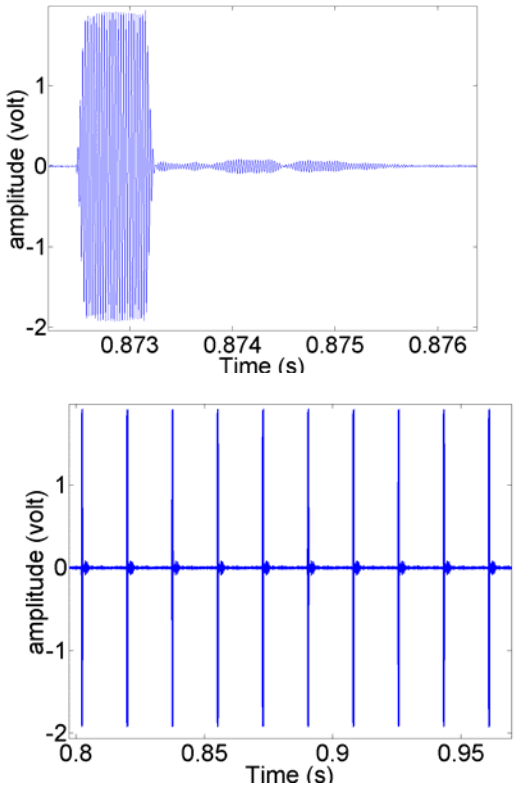

Figure 14. Time dependence of acoustic pressure, illustrating spaced tone bursts at two different time resolutions. Top image shows a detail of a single burst, illustrating subsequent echoes.

Obtaining good, repeatable data from this facility was challenging because of the strong role of buoyancy effects at these low flow velocities. For example, the downstream nozzle was fitted on the facility after realizing that the CO_2 stream flowed sharply downward out of the box exit, being heavier than the ambient air. This created a low pressure region near the top of the box, setting up a recirculating air flow that penetrated deep inside the facility. In addition, the lighter H_20 molecules stratified vertically in the gravity field. Based upon the unsteadiness which is sometimes observed in our water concentration measurements, we also speculate that unsteady flow structures persist in the box at certain conditions, possibly similar to the buoyancy induced recirculatory flows induced by a temperature induced density gradient. Consequently, we were only able to obtain reasonable data under relatively limited conditions where the water concentration remained relatively steady.

Although a number of issues related to obtaining good, "clean" measurements still need to be worked out, our data indicates that the proposed technique is capable of discerning different levels of mixedness. Figure 15 illustrates the amplitude of 30 - 60 kHz acoustic signals upon distance between the box and transducer. It shows the monotonic decrease in acoustic amplitude with increasing distance (corresponding to increased mixedness). The amplitude of the errorbar corresponds to the fluctuation level of the signal. In agreement with the predictions in Figure 9 and Figure 10, the sensitivity grows with frequency.

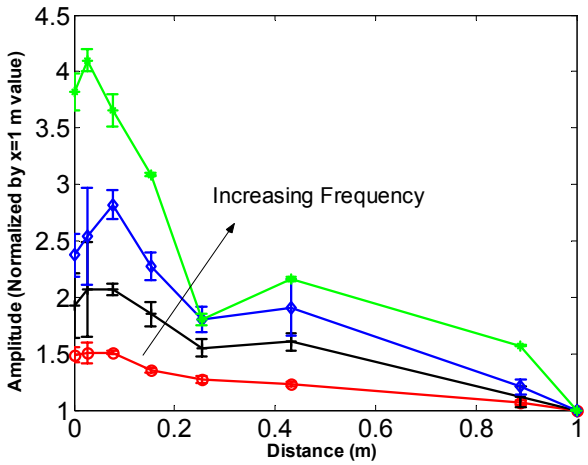

Figure 15. Dependence of 30, 40, 50, and 60 kHz amplitude signal upon axial distance between gas stream origination point and acoustic transducer.

This enhanced sensitivity can also be seen in Figure 16, which plots the ratio of the acoustic amplitude at the x=0 and x=1 m locations as a function of frequency. As above, the errorbar indicates the level of fluctuation of the signal amplitude. Having measured the actual water concentration along the sensor line of sight, we have also plotted the theoretical value of this ratio. It can be seen that the overall measured and predicted trends are in reasonable agreement. Another result at another set of test conditions is shown in Figure 17 . It can be seen that the basic trends are qualitatively similar, but disagree in actual value at the higher frequencies.

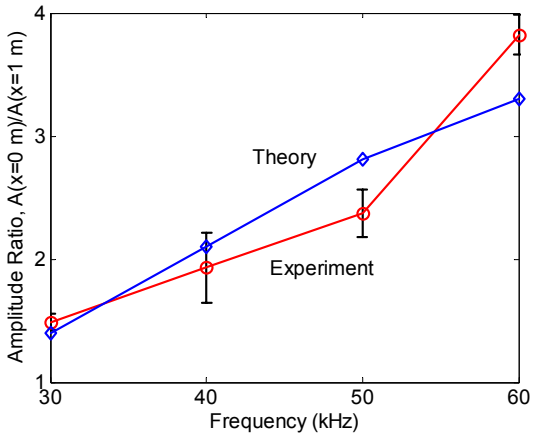

Figure 16. Comparison of theoretical (based upon measured water concentration at box exit) and measured amplitude ratio between unmixed and fully mixed cases (theory based upon measured initial and final concentrations, 0.043% and 0.0075%, respectively).

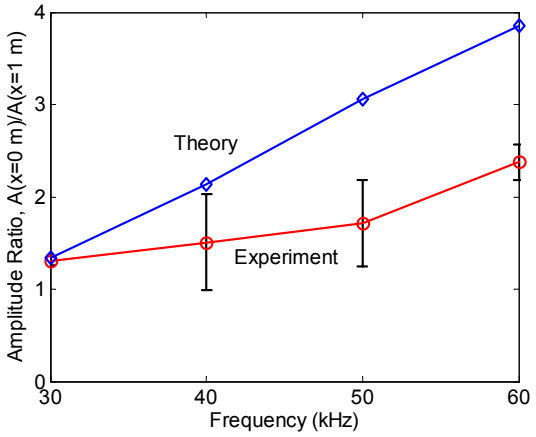

Figure 17. Comparison of theoretical (based upon measured water concentration at box exit) and measured amplitude ratio between unmixed and fully mixed cases (theory based upon measured initial and final concentrations, 0.039% and 0.019%, respectively).

Concluding Remarks

This paper has shown the feasibility of acoustic absorption based measurements as a diagnostic of gas-phase mixing. Measurements have confirmed the variation in absorption levels with mixedness. Further measurements are needed to better characterize the technique, however, and to assess the accuracy with which the "mixedness profile" can be inverted.

1Bhatia, A., *Ultrasonic Absorption*, Dover Publications: New York, 1967.

2 Pierce, A., *Acoustics: An Introduction to its Physical Principles and Applications*, Acoustical Society of America: New York, 1991.

3 Millikan, R., White, D., Vibrational Energy Exchange Between N_2 and CO. The Vibrational Relaxation of Nitrogen, *J. Chem. Phys*., Vol. 39(7), 1963, pp. 1803-1808.

4 Bauer, H., Roesler, H., Relaxation of the Vibrational Degrees of Freedom in Binary Mixtures of Diatomic Gases, in *Molecular Relaxation Processes*, Academic Press: New York, 1966.

5 White., D., Millikan, R., Vibrational Relaxation of Oxygen, *J. Chem. Phys*., Vol. 39(1), 1961, pp. 98-101.

6 White, D., Millikan, R., Vibrational Relaxation in Air, *AIAA J.*, Vol. 2, 1965 pp, 1844-1846.

7 Von Rosenberg, C., Taylor, R., Teare, J., Vibrational Relaxation of CO in Nonequilibrium Nozzle Flow, and the Effect of Hydrogen Atoms on CO Relaxation, *J. Chem. Phys*., Vol. 54(5), pp. 1974-1987.

8 Cottrell, T., Day, M., The Effect of Noble Gases on Vibrational Relaxation in Carbon Dioxide, in Molecular Relaxation Processes, Academic Press: New York, 1966.

9 Knudsen, V., Fricke, E.*, J. Acoust. Soc. Am*., Vol. 5, Vol. 12, 1940, p. 255

10 Nelder, J.A, Mead, R., Simplex Method for Function Minimization, *Comp. J*., Vol. 7, 1965, pp. 308-313.

11 Press, W.H., Teukolsky, S.A., Vetterling, W.T., Flannery, B.P., *Numerical Recipes*, 2nd ed., Cambridge University Press, Cambridge, 1992.